NeuroImage: Clinical 18 (2018) 533–542

Contents lists available at ScienceDirect

NeuroImage: Clinical

journal homepage: www.elsevier.com/locate/ynicl

Neural mechanisms underlying successful and deficient multi-component behavior in early adolescent ADHD

Annet Bluschke[1], Krutika Gohil[1], Maxi Petzold, Veit Roessner, Christian Beste*

Cognitive Neurophysiology, Department of Child and Adolescent Psychiatry, Faculty of Medicine, TU Dresden, Germany

ARTICLE INFO

Keywords:
ADHD
Cognitive control
Neurophysiology
Event related potential (ERP)
Multi-component behavior, inferior parietal cortex

ABSTRACT

Attention Deficit Hyperactivity Disorder (ADHD) is a disorder affecting cognitive control. These functions are important to achieve goals when different actions need to be executed in close succession. This type of multi-component behavior, which often further requires the processing of information from different modalities, is important for everyday activities. Yet, possible changes in neurophysiological mechanisms have not been investigated in adolescent ADHD. We examined N = 31 adolescent ADHD patients and N = 35 healthy controls (HC) in two Stop-Change experiments using either uni-modal or bi-modal stimuli to trigger stop and change processes. These stimuli were either presented together (SCD0) or in close succession of 300 milliseconds (SCD300). Using event-related potentials (ERP), EEG data decomposition and source localization we analyzed neural processes and functional neuroanatomical correlates of multicomponent behavior. Compared to HCs, ADHD patients had longer reaction times and higher error rates when Stop and Change stimuli were presented in close succession (SCD300), but not when presented together (SCD0). This effect was evident in the uni-modal and bi-modal experiment and is reflected by neurophysiological processes reflecting response selection mechanisms in the inferior parietal cortex (BA40). These processes were only detectable after accounting for intra-individual variability in neurophysiological data; i.e. there were no effects in standard ERPs. Multi-component behavior is not always deficient in ADHD. Rather, modulations in multi-component behavior depend on a critical temporal integration window during response selection which is associated with functioning of the inferior parietal cortex. This window is smaller than in HCs and independent of the complexity of sensory input.

1. Introduction

Attention Deficit Hyperactivity Disorder (ADHD) is a prevalent neuropsychiatric disorder in childhood and adolescence (Thomas et al., 2015). It is associated with a number of cognitive dysfunctions including deficits in cognitive control (Gohil et al., 2017a; Heinrich et al., 2017; Nejati et al., 2017; Sebastian et al., 2014; Sonuga-Barke et al., 2016; Tao et al., 2017). Cognitive control functions are especially important for achieving goals when different, separate actions have to be executed in close succession. Often, this requires that an ongoing action has to be interrupted and replaced by an alternative action. These processes can be observed in everyday activities and require a hierarchical organization and processing of several individual actions (Dippel and Beste, 2015). Multi-component behavior (Duncan, 2010; Mückschel et al., 2014) is defined as the processing, prioritizing and integration of multiple actions, such as having a conversation while driving a bike (Duncan, 2010; Mackie et al., 2013; Mückschel et al., 2015, 2014; Stock et al., 2014; Wu et al., 2017). Despite being highly important for day-to-day activities, the underlying neural mechanisms have not been investigated in adolescent ADHD.

Since multi-component behavior often incorporates stopping (interrupting) and changing responses, it requires cognitive processes well-known to be dysfunctional in ADHD; i.e. inhibition (Bluschke et al., 2016; Kenemans et al., 2005; Rommel et al., 2017; Tye et al., 2014) and switching (Kenemans et al., 2005). Crucially, from studies focussing on either stopping or switching processes in ADHD it is not possible to infer how a combination of these processes is modulated in ADHD. This, however, is important since many everyday activities actually require a combination of these processes. Further reason to assume that multi-component behavior is changed in ADHD comes from studies showing that medial frontal, basal ganglia and inferior parietal structures play a central role in multi-component behavior (Beste and Saft, 2015; Mückschel et al., 2014; Ness and Beste, 2013). All of these structures show structural and functional changes in ADHD (Bos et al.,

* Corresponding author at: Cognitive Neurophysiology, Department of Child and Adolescent Psychiatry, Faculty of Medicine, TU Dresden, Schubertstrasse 42, D-01309 Dresden, Germany.
E-mail address: christian.beste@uniklinikum-dresden.de (C. Beste).
[1] Contributed equally.

https://doi.org/10.1016/j.nicl.2018.02.024
Received 10 December 2017; Received in revised form 22 February 2018; Accepted 25 February 2018
Available online 27 February 2018

2017; Brieber et al., 2007; Hoogman et al., 2017) corroborating the assumption that multi-component behavior is changed in ADHD. In fact, there is evidence that multi-component behavior is altered in adult ADHD (Bekker et al., 2005). However, the neurophysiological mechanisms are elusive and nothing is known about adolescent ADHD. This is central, because it has been shown that response selection processes during multi-component behavior are reflected by modulations of the P3 event-related potential (ERP)-component originating in medial frontal and inferior parietal cortices (Beste et al., 2014; Dippel and Beste, 2015; Mückschel et al., 2014; Stock et al., 2014). Importantly, the developmental trajectories of these response selection processes have been shown to be qualitatively different in individuals with ADHD (Downes et al., 2017). The development of various P3 characteristics has been shown to differ between patients with ADHD and healthy controls (Downes et al., 2017) and especially the developmental trajectories of inhibitory control seem to differ significantly between individuals with and without ADHD (Doehnert et al., 2013). Together, these considerations about known cognitive deficits and neuroanatomical peculiarities in ADHD make it likely that there are deficits in multi-component behavior in ADHD compared to healthy adolescents. However, the magnitude of this difference between early adolescent ADHD and healthy controls may be crucially influenced by two factors, which were not considered in existing data on multi-component behavior in ADHD (Bekker et al., 2005):

Firstly, there seems to be a critical “window” of time within which separate stimuli are very likely to become integrated (Conrey and Pisoni, 2006; Diederich and Colonius, 2009; Meredith, 2002; van Wassenhove et al., 2007). This is crucial in the context of multi-component behavior, since different stimuli need to be integrated to execute separate task goals to produce an efficient goal-directed behavior. Critically, it has recently been shown that multi-component behavior in healthy adolescents becomes particularly difficult when temporally separated stimuli have to be integrated during response selection (Gohil et al., 2017b). Notably, in individuals with ADHD, the temporal gaps upon which stimuli can still be integrated are considerably shorter (Marusich and Gilden, 2014). Therefore, ADHD patients may show deficits compared to healthy controls, when stimuli signalling two to be cascaded actions are presented with a gap in time between the stimuli.

Secondly, multi-component behaviour changes significantly when it is necessary to integrate information from different sensory modalities. This may be a particularly relevant issue given the significant sensory processing problems in ADHD (Dionne-Dostie et al., 2015). However, existing results show that sensory processes do not directly modulate multi-component behavior, but exert their effects via the modulation of response selection processes (Gohil et al., 2015).

In the current study we focus on these potentially important modulators of multi-component behavior in early adolescent ADHD. This is done using a system neurophysiological approach where we delineate alterations in cognitive-neurophysiological processes using ERPs and source localization methods. The latter are used to delineate the functional neuroanatomical networks associated with the modulations in multi-component behavior. It is hypothesized that behavioral and neurophysiological differences in multi-component behaviour are present between adolescent ADHD patients and controls. Specifically, we expect that these differences are particularly strong when stimuli signalling how different executive processes are temporally separated. That is ADHD patients and controls may differ from each other when two to be cascaded actions are signalled in a step-by-step fashion, but not when they are signalled simultaneously. If the number of modalities is further critical to consider, these differences are more pronounced when multi-component behavior is signalled via different sensory modalities. To examine these important aspects of multi-component behavior, we used a ‘stop-change task’ (SCT). This task requires participants to occasionally interrupt (stop) an ongoing response in favour of an alternative response (change). Importantly, the signal to execute the alternative response is either presented at the same time, or with a short delay. Moreover, the STOP and the CHANGE signals are varied in their modalities in two experiments – one experiment uses visual STOP and visual CHANGE stimuli. The other experiment uses visual STOP and auditory CHANGE stimuli.

Regarding neurophysiological processes underlying above-mentioned modulations it is crucial to note that intra-individual variability, known to be strong in ADHD (Henríquez-Henríquez et al., 2014; Lin et al., 2015; Saville et al., 2015), can mask difficulties in response selection processes in ADHD and the detection of their neurophysiological and functional neuroanatomical underpinnings (Bluschke et al., 2017). It has been shown that the ERP method can only yield accurate insights into the neurophysiological processes of cognitive functions when there is little intra-individual variability (Ouyang et al., 2011). It follows that when such data is used in subsequent source localization analyses, these problems likely affect our knowledge about functional neuroanatomical structures associated with the cognitive processes examined (Bodmer et al., 2017). This is especially the case for neurophysiological correlates of response selection processes (such as the P3 ERP component) (Ouyang et al., 2015a, 2017; Verleger et al., 2014). These processes are expected to be modulated in ADHD. This is also because previous studies have consistently shown that response selection processes during multi-component behavior (examined using the SCT) are reflected by modulations of the P3 (Beste et al., 2014; Dippel and Beste, 2015; Mückschel et al., 2014). Therefore, we apply residue iteration decomposition (RIDE) to the data (Ouyang et al., 2015b, 2015a, 2011). This method produces three component clusters with dissociable functional relevance (Ouyang et al., 2011): the S-cluster refers to processes related to perception and attention, the R-cluster refers to processes related to the response (such as motor preparation and execution) and the C-cluster refers to intermediate processes such as response selection (Ouyang et al., 2011). Recent results show that particularly processes reflected by the C-cluster are modulated in ADHD (Bluschke et al., 2017) and that the C-cluster reflects the same processes that are reflected by the P3 ERP (Verleger et al., 2014). Therefore, we hypothesize that deficits in multi-component behavior in early adolescent ADHD are reflected by reductions in the C-cluster amplitude, particularly when temporally separated stimuli need to be used. These modulations are expected to be associated with the inferior parietal cortex as suggested by previous studies (Wolff et al., 2017), also because this cortical area plays an important role in multi-component behavior (Duncan, 2010). No, or little modulations are expected for the S-cluster and R-cluster data.

2. Materials and methods

2.1. Participants

All parents of the participants provided written informed consent according to the Declaration of Helsinki and the study was approved by the local ethics committee of the Medical Faculty of the TU Dresden. Early adolescent ADHD patients (N = 35) according to ICD-10 criteria were recruited from our outpatient clinic. Standard clinical procedures (including parent and child interview, teacher report, symptom questionnaires, IQ testing, exclusion of potential underlying somatic disorders via EEG, ECG, audiometry and vision testing) had been used to confirm the ADHD diagnosis in the clinical setting. Fourteen patients were taking medication (methylphenidate, lisdexamphetamine, atomoxetine). Four patients were excluded during data analyses due to poor EEG data quality (i.e. Muscle artefacts and excessive movements) so that n = 31 patients (12.64 years ± 1.76 (10–14 years); 2 females) remained in the sample. To measure ADHD symptoms at the time of testing, the patient's parents or legal guardians completed the German ADHD rating scale (Döpfner et al., 2008). Here, a rating between 0 and 3 was given concerning the diagnostic criteria of ADHD with an average rating above 1.5 indicating highly clinically significant symptoms. In sum, parents rated the behaviour of their children regarding inattention

(1.74 ± 0.72), hyperactivity (0.89 ± 0.66) and impulsivity (1.66 ± 0.71), thus confirming that recruited children showed attention-related problems. General intelligence was examined using the "Hamburg-Wechsler-Intelligenztest für Kinder" (HAWIK) (IQ 100.8 ± 12.6). Early adolescent healthy children (N = 35; 12.55 ± 1.55 years (10–14 years); 2 females) recruited from an in-house database participated as controls. None of them had to be excluded due to poor EEG data quality. The controls did not differ from the ADHD patients in regards to IQ and age ($p > 0.6$). Therefore, age or IQ were not included as a covariate in the statistical analyses. All testings were performed in the afternoon (~4 pm). Due to the short half-life of medication (~ 4 h) and drug intake in the morning at ~7 am, this should only have a minimal effect in the ADHD group.

The initial sample size was calculated in G*power under the assumption of a medium effect size f = 0.25 and the statistical model used to analyze the data (refer statistics section). The power analysis revealed that a power > 95% is achieved using a total sample size of N = 54. Since we enrolled N = 70 participants (N = 35 patients and N = 35 controls), the study was well-powered even after removing N = 4 ADHD patients from data analysis as described above.

2.2. Task

2.2.1. Experimental paradigms (tasks)

A modified version of the Stop-Change paradigm introduced by (Verbruggen et al., 2008) was used in this study (see Figure below for illustration) and is shown in Fig. 1. The paradigm is identical to a previous study (Gohil et al., 2017b).

All participants were comfortably seated in front of a 17 in. CRT computer monitor at a distance of 57 cm. A regular computer keyboard was placed in front of the participants and they were instructed to press one out of four different keys (letters "S," "C," "N," and "K") in each trial to correctly respond. The participants were asked to respond with both hands (i.e. "S"/"C" using the left hand and "N"/"K" using their right hand). The participants performed the task with 576 trials. Two thirds were "GO" trials and the rest were "Stop-Change" (SC) trials. The trial order was pseudo-randomized. The task array was presented on a black background (0.4 cd/m^2). As shown in the figure, it consisted of a white bordered rectangle which contained 2 vertically arranged circles with white borders and three white horizontal lines (width 13 mm, line thickness 1 mm). This empty array was presented at the beginning of each trial for 250 ms before one of the three circles (diameter of 7 mm) was filled in with white color (120.1 cd/m^2), thus becoming the target stimulus in the GO condition. Of note, the GO stimulus remained on the screen until the end of the trial. Participants had to respond with their right middle finger ("K" key) when the target was located above the middle white line, and to respond with their right index finger ("N" key) when the target was located below the middle line. If the participants failed to respond within 1000 ms after the target stimulus onset, a sign asking to speed up responses (the German word "Schneller!" which translates to "Faster!") appeared above the stimulus array. This sign remained on the screen until the trial was ended by a button press.

Stop-Change (SC) trials occurred with a likelihood of 33%. These SC trials also began with the empty array followed by the GO stimulus. During the SC trials, a STOP stimulus (the white rectangle border turning red, see Figure) was presented after the GO stimulus with a variable Stop-signal delay (SSD). This STOP stimulus as well as the GO stimulus remained on the screen until the end of the SC trial because the position of the target/GO stimulus in relation to one of the three horizontal lines had to be re-evaluated upon the presentation of the CHANGE stimulus. The SSD was adjusted to each participant's individual task performance using a staircase algorithm throughout the experiment (Verbruggen et al., 2008): The SSD was initially set to 250 ms. When the participant did not press a key before the presentation of the STOP stimulus and correctly responded to the CHANGE stimulus as described below during an SC trial, the SSD was increased by 50 ms. In contrast to this, any incorrect responses (i.e. responses within the SSD/before the CHANGE stimulus as well as wrong responses to the CHANGE stimulus) decreased the SSD by 50 ms. As a result, the staircase procedure produced a 50% probability of successfully performed SC trials in case participants correctly followed the task instructions. The SSD variation was restricted to range from 50 to 1000 ms to keep the trial duration within reasonable limits.

All participants completed a visual and a visual-auditory version of the Stop-Change paradigm. A CHANGE stimulus was presented after the STOP stimulus and required the participants to respond with their left hand. The reaction time (RT) was measured relative to the presentation of this CHANGE stimulus. There were two SC conditions. In the first

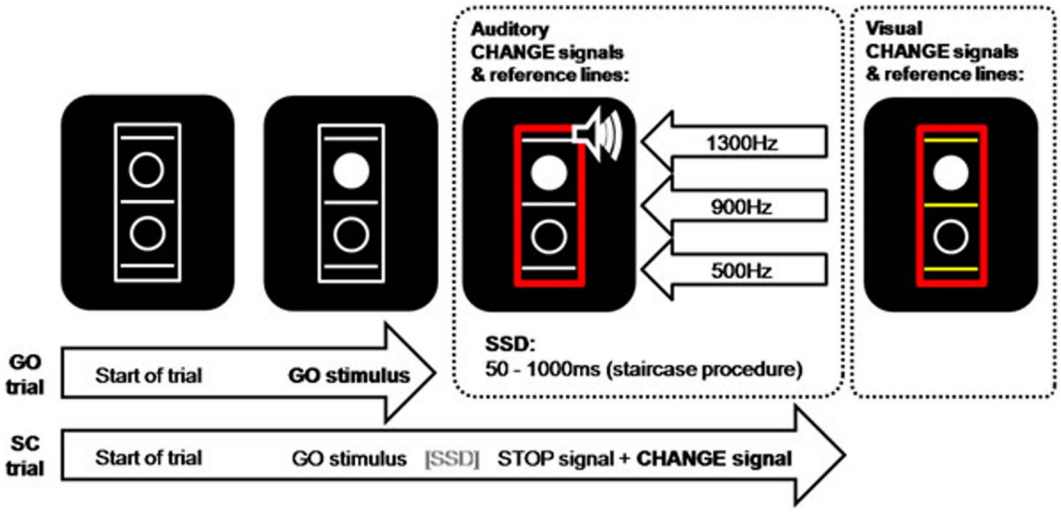

Fig. 1. Schematical illustration of the experimental setup. Participants were presented with a visual GO signal (white circle) above or below a central horizontal line at the beginning of all trials. In GO trials, the subjects needed to respond with the right hand (middle finger = "above" response, index finger = "below" response). In stop-change trials, the GO stimulus was followed by a visual STOP stimulus (red rectangle, see middle) after a variable and individually adjusted stop-signal delay (SSD). The CHANGE stimulus was either presented with a stimulus onset asynchrony (SOA)/stop-signal delay (SCD) of 0 ms or of 300 ms after the STOP stimulus. The CHANGE stimulus now indicated that the response needed to be made with the left hand. In the unimodal task, the CHANGE stimulus was a bold yellow line. By contrast, the bimodal task used 200 ms sine tones (1300 Hz, 900 Hz, and 500 Hz) as CHANGE stimuli. Participants were thus required to change their response according to the new indicated line (middle finger = "above" response, index finger = "below" response) or the pitch of the tone (middle finger = "high pitch", index finger = "low pitch").

condition, there was no Stop-Change delay (SCD0) so that STOP and CHANGE stimuli were presented at the same time. The second SC condition had a stimulus onset asynchrony of 300 ms (SCD300) so that the CHANGE stimulus always followed the onset of the STOP stimulus after 300 ms. This stimulus onset asynchrony was chosen because the stopping process is then finished before the CHANGE process can be initiated upon presentation of the CHANGE stimulus (Gohil et al., 2017b). In the SCD300-condition, sub-tasks are therefore separated resulting in a lower overlap of STOP and CHANGE-related processes making the SCD300 condition easier than the SCD0 condition (Letzner et al., 2017). Regardless of the stimulus modality, the CHANGE stimuli point out one of the three lines to the participants who were instructed to spatially relate the target (i.e. the white circle) to the new reference line. Participants were instructed to respond with their left hand middle finger ("S" key) when the target was located above the newly set reference line, and to respond with their left hand index finger ("C" key) when the target was located below the newly set reference line. If participants did not respond within 2000 ms after the onset of the CHANGE stimulus, the speed up sign appeared above the stimulus array and stayed on the screen until the trial was terminated by a button press. As with the SCD0 trials, the RT is timed from the Change stimulus on. However, there is not is a more restricted time window for responding on the SCD300 trials, compared with the SCD0, because this could induce cognitive effects aside from the temporal binding and the multisensory processing. The dominant right hand was always used to respond to the GO stimuli because it responds faster than the non-dominant hand, which makes stopping the initial GO response a bit more demanding (although this aspect is minimized due to the applied staircase procedure). The reason why the other hand was used for CHANGE stimuli is that it makes the CHANGE more demanding.

2.2.2. Visual and auditory experiments

In the visual version of the experiment, the CHANGE stimuli were bold yellow bars presented for 200 ms replacing one of the three white lines, thus turning it into the new reference line. In the visual-auditory version of the experiment, a sine tone (200 ms duration), which was presented via headphones to both ears, was used as the CHANGE stimulus. In each SC trial, one of three differently pitched tones (low/500 Hz, middle/900 Hz, and high/1200 Hz) was presented at a 75 dB sound pressure level. Prior to the testing we ensured that each of the different pitches could be discriminated with at least 95% accuracy. Importantly, this included that not only the pitch could be distinguished but that also the association with the different lines of the visual array as outlined below, which required training the ADHD and the control group.

Each tone represented one of the three horizontal lines (i.e. the high 1200 Hz tone represented the high reference line, the middle 900 Hz tone represented the middle reference line, and the low 500 Hz tone represented the low reference line). The auditory CHANGE required the participants to take both the visual information and the auditory information into account to perform a correct response. For example, a filled white circle right below the middle line required an "above" judgement when the CHANGE stimulus was the low tone (500 Hz), but a "below" judgement whenever the CHANGE stimulus was the high tone (1200 Hz). This should illustrate that neither information alone (i.e. auditory or visual) was sufficient to come up with the correct response. Instead, both the information of the STOP and the CHANGE stimuli (i.e. uni-modal visual, or bi-modal visual-auditory information) need to be integrated to reach a valid decision which response to execute. Importantly, the GO stimulus was still displayed, when the CHANGE stimuli was presented. The concept of the temporal window of integration refers to the window in which concurrent multisensory information can be integrated into one percept or can exert a cross-modal influence. This is the case in the paradigm applied.

2.2.3. Neurophysiological data analysis

A QuickAmp amplifier (Brain Products, Inc.) connected to 60 sintered Ag/AgCl electrodes located at equidistant scalp positions (customized BrainCap Fast'n Easy sub-inion model EEG caps) using the 10/10 system nomenclature was used to acquire a high-density EEG recording (500 Hz sampling rate) with Fpz as reference electrode (electrode impedances $< 5\,k\Omega$). Offline, the EEG was down-sampled to 256 Hz before applying an IIR band-pass filter ranging from 0.5 to 20 Hz (with a slope of 48 db/oct each) using the BrainVision Analyzer 2 software package. This was followed by a manual raw data inspection to remove rare motor artifacts such as sneezing or jaw-clenching. Afterwards, an independent component analysis (ICA) using the Infomax algorithm was applied to remove the regular/recurring artifacts like eye blinks or saccades. The number of ICs removed varied between 3 and 10 (mean = 4.8 ± 2.8). Subsequently, single-trial segments locked to the onset of the visual STOP stimulus were formed for the two SCD conditions. Each of the segments started -900 ms before the onset of the STOP stimulus (set to time point zero) and ended 1200 ms thereafter. Only correct trials were included in the data analysis, i.e. where the GO response was successfully interrupted and the correct response to the CHANGE stimulus was executed. Then, an automated artifact rejection procedure was applied and the rejection criteria were: (i) value difference of $> 150\,\mu V$ in a 250 ms interval, (ii) activity below $0.1\,\mu V$ in a 200 ms interval, (iii) a maximum voltage step of $> 60\,\mu V$/ms. The artifact rejection procedure eliminated ~2.1% (± 1.5) of trials not differing between groups and experimental conditions. Following this, a current source density (CSD), transformation was applied (Nunez and Pilgreen, 1991), which reduces the spreading of electrical activity across electrodes sites and helps identify the electrodes that best reflect neurophysiological activity related to specific cognitive processes. Then, a baseline correction was applied in the time window from −900 till −700 ms. This time window was chosen to have a 'real' pre-stimulus baseline that was well before the presentation of the GO stimulus (Mückschel et al., 2014). Lastly, the single trial segments were individually averaged for each SC condition. Based on this procedure, the P1, N1 and P3 ERPs mean amplitudes were quantified. Electrodes and components were chosen based on a visual inspection of the scalp topography of the grand average over participants and conditions. Based on this, the visual P1 and N1 ERPs (i.e. mean amplitudes) on the STOP stimulus were quantified at electrodes P7 and P8 (P1:110–130 ms and N1: 190–210 ms) in the visual-auditory experiment and the visual-visual experiment. The auditory N1 (i.e. mean amplitudes) on the CHANGE stimulus (in case of the visual-auditory experiment) was quantified at electrodes C5 and C6 (SCD0: 200–230 ms, SCD300: 420–510 ms). The visual N1 on the CHANGE stimulus (i.e. mean amplitudes) (in case of the visual-visual experiment) was quantified at electrodes P7 and P8 (SCD0: 190–230 ms, SCD300: 420–510 ms). The P3 (i.e. mean amplitudes) was quantified at electrode Cz (SCD0: 270–330 ms, SCD300: 540–580 ms) in the visual-auditory experiment and the visual-visual experiment. The electrodes and time windows used for data quantification were chosen by visual inspection of the scalp topography plots. This choice of electrodes and time windows was validated using statistical methods (Mückschel et al., 2014): Within each of these search intervals (see above), the peak amplitude was extracted for all electrodes. Each electrode was subsequently compared against the average of all other electrodes using Bonferroni-correction for multiple comparisons (critical threshold $p = 0.0007$). Only electrodes that showed significantly larger mean amplitudes (i.e., negative for N-potentials and positive for the P-potentials) than the remaining electrodes were selected. This procedure revealed the same electrodes as previously chosen by visual inspection. The quantification of all ERPs was made at the single subject level. Latency windows for data quantification are given relative to the onset of the stop signal (time point 0), and amplitudes were quantified relative to the pre-stimulus baseline.

2.2.4. Residue Iteration Decomposition (RIDE)

Residue iteration decomposition (RIDE) was performed to account for effects of intra-individual variability. This particular important in the ADHD, which has previously been shown to reveal a high intra-individual variability, which can be captured using RIDE (Bluschke et al., 2017). Algorithms from the RIDE toolbox were applied according to established procedures(Ouyang et al., 2011): RIDE is applied on the segmented single-trial data for each participant/patients separately. RIDE uses the timing and timing variability properties of the EEG signal to decompose this data. Since this done for each channel separately (Ouyang et al., 2011), the application of the CSD transformation (or reference in general) is not critical for the RIDE estimation procedure. As already described by Bluschke et al. (2017); to quote: "The time markers ("latencies") used for deriving the S and R cluster components ("LS" and "LR") are the time points of the stimulus and response onsets, respectively. In contrast to this, the time markers for deriving C ("LC") are estimated and iteratively improved. RIDE uses a time window function to extract the waveform of each RIDE component. For the current study this was from 200 ms prior to target to 600 ms after the target for the S-cluster, from 200 to 900 ms after the target for the C-cluster and ± 300 ms around the response trigger for the R-cluster. To estimate S, RIDE subtracts C and R from each single trial and aligns the residual of all trials to the latency "LS" in order to obtain S as the median waveform for all time points. The equivalent procedure is applied to obtain C and R. For the R-cluster the response needs to be part of the epoch and around 98% of all responses were carried out within the epoch. The whole procedure is iterated to improve the estimation of the components until they converge (criterion: $< 10^{-3}$ difference for the values of two successive iterations). Full details on the RIDE method can be found in (Ouyang et al., 2015b)."

After estimating the different RIDE clusters, amplitudes of each cluster were quantified in specific time windows: The S-cluster was quantified at electrodes TP7 and TP8 to examine P1/N1-releated processes on the auditory CHANGE stimuli in the visual-auditory experiment. In the SCD0 condition this was done between 110 ms and 130 ms for the P1 and between 190 ms and 205 ms for the N1. In the SCD300 condition this was done between 440 ms and 450 ms for the P1 and between 490 ms and 510 ms for the N1. For the visual STOP stimuli the S-cluster was quantified at electrodes P7 and P8 in the visual-visual and visual-auditory experiment between 105 ms and 120 ms for the P1 and between 205 ms and 220 ms for the N1 (for the SCD0 and SCD300 condition). In the SCD300 condition, the CHANGE stimuli in the S-cluster was quantified between 440 and 450 ms for the P1 and between 490 and 510 ms for the N1 in the uni-modal and bi-modal experiment. In the uni-modal (visual CHANGE stimuli) this was done at electrode P7 and P8. In the bi-modal experiment (auditory CHANGE stimuli) this was done at electrode TP7 and TP8. Moreover, the S-cluster was quantified at electrode Cz between 220 ms and 240 ms in the SCD0 condition and between 520 ms and 540 ms in the SCD300 condition. The C-cluster was quantified at electrode Cz and CP4. In the SCD0 condition, mean amplitudes were quantified between 610 ms and 650 ms for electrode Cz and CP4. In the SCD300 condition mean amplitudes were quantified between 610 ms and 650 ms at electrode CP4 and between 450 ms and 490 ms at electrode Cz. The R-cluster was quantified at electrode C4, because the responses on the CHANGE stimuli were always executed with the left hand. In the SCD0 condition, in this was done between 1140 ms and 1200 ms, in the SCD300 condition this was done between 1250 ms and 1310 ms. The choice of time windows and electrodes chosen for data quantification in the different RIDE clusters were also validated using the statistical approach outlined in (Mückschel et al., 2014), which was also used for the standard ERP data.

2.2.5. sLORETA

We used the estimated RIDE clusters as a basis for the source localization analysis, as done in previous studies (Wolff et al., 2017). sLORETA (standardized low resolution brain electromagnetic tomography; (Pascual-Marqui, 2002) was conducted for source localization. It provides a single linear solution for the inverse problem without localization bias (Marco-Pallarés et al., 2005; Sekihara et al., 2005). The method shows high convergence with fMRI data (Sekihara et al., 2005). EEG/TMS-studies further confirm the validity of sources estimated with sLORETA (Dippel and Beste, 2015). The MNI152 template was used for the calculation of the standardized current density at each voxel (Fuchs et al., 2002). These voxel – based sLORETA images (6239 voxels at 5 mm spatial resolution) of the intracerebral volume were compared between the two groups. For comparing the groups, the sLORETA – built – in voxel – wise randomization test with 2000 permutations was used ($p < 0.01$, corrected for multiple comparisons) based on statistical nonparametric mapping. Significant differences between voxels in contrasted conditions were located in the MNI brain (www.unizh.ch/keyinst/NewLORETA/sLORETA/sLORETA.htm).

2.2.6. Statistics

To analyze behavioral and neurophysiological data (i.e. ERP and RIDE-cluster data), separate mixed effects analyses of variance (ANOVAs) were used. The factors "SCD interval" (SCD0 vs. SCD300) and "modality" (uni-modal vs. bi-modal SC stimuli) were used as within-subject factors. "Group" (ADHD vs. controls) was used as a between-subjects factor. Greenhouse-Geisser correction and Bonferroni-correction was conducted. Kolmogorov–Smirnov tests indicated that all variables used for the analysis were normally distributed (all $z < 0.9$; $p > 0.6$). For all descriptive statistics, the standard error of the mean (SEM) was used as a measure of variability. For non-significant results including the factor "group" we also run Bayesian analyses to examine the probability of the null hypothesis being true, given the obtained data ($p(H_0|D)$ (Masson, 2011; Wagenmakers, 2007); i.e. we evaluate the relative strength of evidence for the null hypothesis. The Bayesian analysis was performed on the basis of the sum of squares of the error term and the effect term provided by the ANOVAs (Masson, 2011; Wagenmakers, 2007).

3. Results

3.1. Behavioral data

For the reaction time (RT) data on GO trials, there was a main effect "modality" ($F(1,64) = 9.46$; $p = 0.003$; $\eta_p^2 = 0.129$) showing that RTs were longer in the bi-modal (734 ms ± 22) than the uni-modal condition (673 ms ± 14). There were no other main or interaction effects, also not for the accuracy data (all $F < 0.7$; $p > 0.3$).

On Stop-Change (SC) trials, and for the RTs on CHANGE stimuli, the mixed effects ANOVA revealed a main effect "SCD interval" ($F(1,64) = 89.91$; $p < 0.001$; $\eta_p^2 = 0.584$) showing that RTs were slower in the SCD0 condition (1108 ms ± 19) than in the SCD300 condition (953 ms ± 19). The main effect "modality" ($F(1,64) = 74.11$; $p < 0.001$; $\eta_p^2 = 0.537$) showed that RTs were faster in the uni-modal (883 ms ± 21) than in the bi-modal experiment (1178 ms ± 27). There was an interaction of "SCD interval x group" ($F(1,64) = 8.22$; $p = 0.006$; $\eta_p^2 = 0.114$), shown in Fig. 2 (top).

Post-hoc tests showed that the groups did not differ in the SCD0 condition ($t(64) = 0.26$; $p = 0.23$), but in the SCD300 condition ($t(64) = 4.01$; $p < 0.001$) where controls showed faster RTs than patients with ADHD. No other main or interaction effects were significant (all $F < 0.12$; $p > 0.86$). The Bayesian analysis supports the lack of effects since $p(H_0|D)$ was larger than 0.81 for all effects, thus providing positive evidence for the null hypothesis according to Raftery's (1995) criteria. Concerning RT variability, the analysis shows only a main effect of "Group" ($F(1,64) = 36.12$; $p < 0.001$; $\eta_p^2 = 0.114$) with variability being larger in patients with ADHD (339 ms ± 30) than in controls (295 ms ± 28). No other main or interaction effect was significant (all $F < 0.24$; $p > 0.7$).

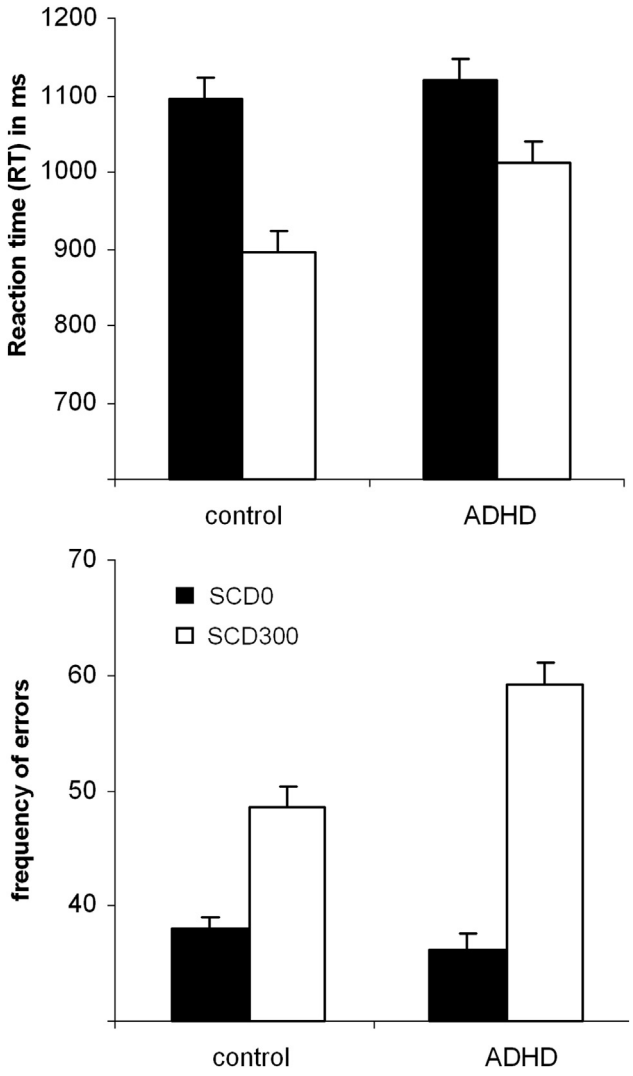

Fig. 2. Behavioral data showing the RTs (top) and the frequency of errors (bottom) for the control and the ADHD group in the SCD0 (black bars) and the SCD300 condition (white bars). The mean and standard error of the mean are given.

Regarding the accuracy (i.e. frequency of error responses on CHANGE trials), the mixed effects ANOVA revealed a main effect of "SCD interval" ($F(1,64) = 451.52$; $p < 0.001$; $\eta_p^2 = 0.876$) with errors being higher in the SCD300 condition (71.8 ± 1.3), than in the SCD0 condition (52.1 ± 0.7). The main effect of "modality" ($F(1,64) = 39.19$; $p < 0.001$; $\eta_p^2 = 0.380$) showed that accuracy was higher in the uni-modal (66.5 ± 1.2) than in the bi-modal experiment (57.3 ± 1.2). There was an interaction between "SCD interval x "Group" ($F(1,64) = 14.41$; $p < 0.001$; $\eta_p^2 = 0.184$), which is also shown in Fig. 2 (bottom). Post-hoc tests showed that the groups did not differ in the SCD0 condition ($t(64) = 0.26$; $p = 0.23$), but in the SCD300 condition ($t(64) = 4.01$; $p < 0.001$) where controls showed better performance (i.e. higher accuracy) than ADHD patients. No other main or interaction effects were significant (all $F < 0.35$; $p > 0.79$). The Bayesian analysis supports the lack of effects and shows that $p(H_0|D)$ was larger than 0.80 for all of these effects.

To control for the effects of medication, the medication status (i.e. the compound used) was used a covariate. These analyses show that the addition of this covariate did not alter the main or interaction effects found in above analyses and there was also no effect of the covariate itself (all $F < 0.55$; $p > 0.7$). It is also shown that the ADHD patients taking medication did not differ from the patients taking no medication, when the ADHD patient group was split (all $F < 0.65$; $p > 0.7$).

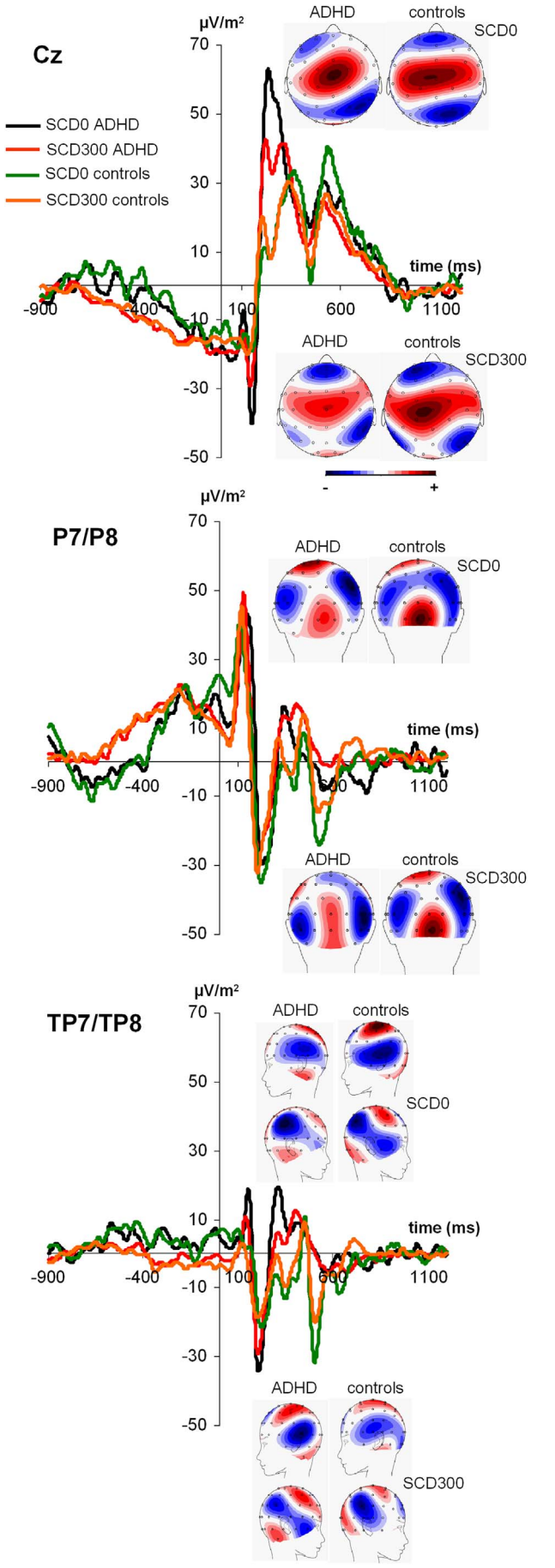

(caption on next page)

Fig. 3. RIDE S-cluster data at electrodes Cz (top), pooled across P7/P8 (middle) and pooled across TP7/TP8 (bottom). The data are shown pooled across the uni-modal and the bi-modal condition, because there was no difference between these conditions. The different colors denote the different experimental conditions (SCD0, SCD300) in combination with the respective group (ADHD, controls). Time point zero denotes the time point of the STOP stimulus presentation. The scalp topographies for the ADHD and the control group are shown for the different condition (SCD0, SCD300). In the scalp topographies, blue colors show negativity, red colors positivity. The topographies are shown for the maximum amplitudes in the respective time windows for peak quantification as outlined in the methods section.

3.2. Neurophysiological data

3.2.1. Standard ERP analysis

The P1 and N1 ERP-components, as well as the P3 ERPs components are shown in the Supplemental material. The mixed effects ANOVAs for these ERP components revealed no main or interaction effects including the factor "group" (all $F < 0.28$; $p > 0.8$) and the Bayesian analysis supports this lack of modulatory effects of the factor "group" showing that $p(H_0|D)$ was larger than 0.80 for all of these effects.

3.2.2. Residue iteration decomposition

The S-cluster data is shown in Fig. 3.

For the S-cluster data, the amplitudes in the P1 and N1 time windows were analyzed in mixed effects ANOVA using the factors "SCD interval" and "stimulus modality" as within-subject factors and "group" as the between-subject factor. The S-cluster in the P1 and N1 time range is shown in Fig. 3 for the visual and auditory P1/N1 in case of auditory CHANGE stimuli in the bi-modal experiment. The factor "electrode" was not modeled because the auditory P1/N1 could only be quantified in the bi-modal task version so that any effect of "electrode" would have been confounded by the stimulus modalities (Gohil et al., 2017b). In the P1 time window this mixed effects ANOVA revealed only an interaction "modality x SCD interval" ($F(1,64) = 5.50$; $p < 0.022$; $\eta_p^2 = 0.079$). All other main or interaction effects were not significant (all $F < 0.16$; $p > 0.69$). For the S-cluster in the N1 time window the mixed effects ANOVA revealed a main effect "SCD interval" ($F(1,64) = 20.64$; $p < 0.001$; $\eta_p^2 = 0.244$), showing that amplitudes were more negative in the SCD300 ($-30.28\,\mu V/m^2 \pm 3.2$) condition than in the SCD0 condition ($-11.43\,\mu V/m^2 \pm 2.3$). No main or interaction effects were significant (all $F < 0.09$; $p > 0.7$). However, the S-cluster was also prominent in the P3 time window at central electrode leads around electrode Cz. For electrode Cz, the mixed effects ANOVA revealed a main effect of "modality" ($F(1,64) = 27.72$; $p < 0.001$; $\eta_p^2 = 0.302$) showing that S-cluster amplitudes were larger in the bi-modal ($49.75\,\mu V/m^2 \pm 5.6$) than the uni-modal condition ($14.87\,\mu V/m^2 \pm 3.1$). The main effect "SCD interval" ($F(1,64) = 4.26$; $p < 0.043$; $\eta_p^2 = 0.062$) showed that the S-cluster amplitude was larger in the SCD0 ($37.31\,\mu V/m^2 \pm 3.2$) condition than in the SCD300 condition ($27.31\,\mu V/m^2 \pm 4.5$). No other main or interaction effects were significant (all $F < 0.21$; $p > 0.8$). The Bayesian analysis supports the lack of group-related main or interaction effects in the S-cluster and shows that $p(H_0|D)$ was larger than 0.85 for all of these effects.

Regarding the C-cluster data, the mixed effects ANOVA revealed a main effect of "electrode" ($F(1,64) = 142.89$; $p < 0.001$; $\eta_p^2 = 0.691$) showing that the C-cluster was negative at electrode Cz ($-20.93\,\mu V/m^2 \pm 3.5$) and positive at electrode CP4 ($24.37\,\mu V/m^2 \pm 1.2$). The main effect of "modality" ($F(1,64) = 8.44$; $p = 0.005$; $\eta_p^2 = 0.117$) revealed that the C-cluster was positive in the uni-modal experiment ($8.09\,\mu V/m^2 \pm 2.3$) and negative in the bi-modal experiment ($-4.66\,\mu V/m^2 \pm 3.3$). The main effect of "SCD interval" ($F(1,64) = 8.16$; $p = 0.006$; $\eta_p^2 = 0.113$) showed that the C-cluster was positive in the SCD300 condition ($5.46\,\mu V/m^2 \pm 1.7$) and negative in the SCD0 condition ($-2.02\,\mu V/m^2 \pm 2.6$). Importantly, there was an interaction of "electrode × SCD interval × group" ($F(1,64) = 4.31$; $p = 0.042$; $\eta_p^2 = 0.063$). No other interaction effects were significant (all $F < 0.15$; $p > 0.69$). The Bayesian analysis supports the lack of effects and shows that $p(H_0|D)$ was larger than 0.83 for all of these effects. The interaction "electrode × SCD interval × group" was analyzed in more detail: For electrode Cz, the interaction "SCD interval × group" was not significant ($F(1,64) = 0.19$; $p = 0.7$), but this was the case for electrode CP4 ($F(1,64) = 8.29$; $p = 0.005$; $\eta_p^2 = 0.115$) (refer Fig. 4).

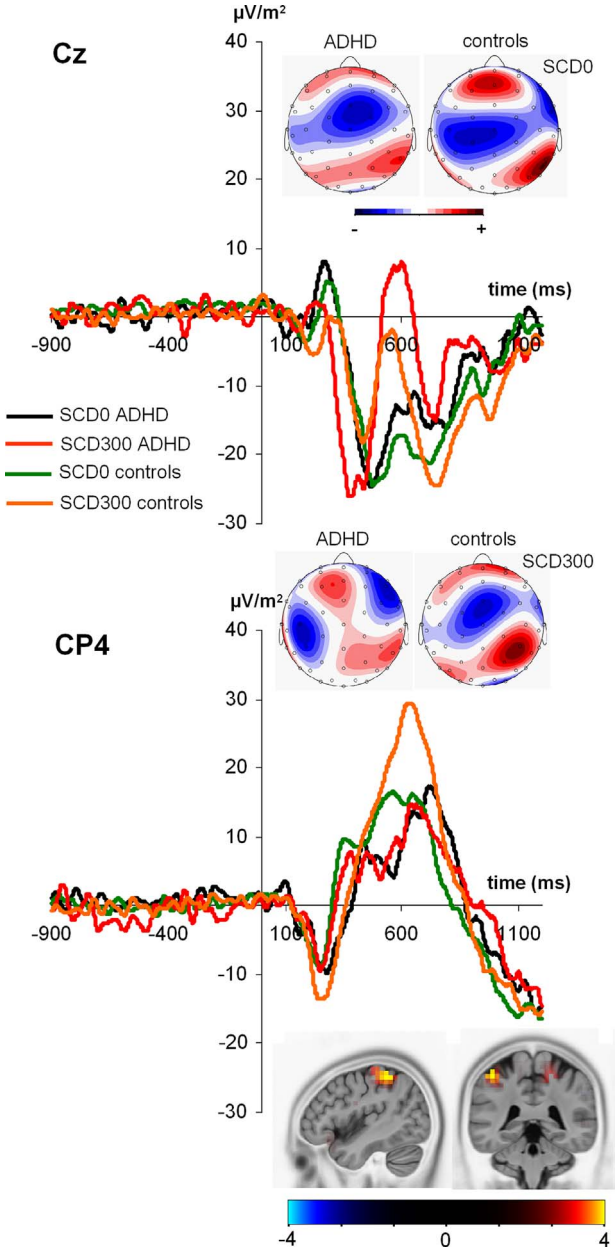

Fig. 4. RIDE C-cluster data at electrodes Cz (top), and CP4 (bottom). The data are shown pooled across the uni-modal and the bi-modal condition. The different line colors denote the different experimental conditions (SCD0, SCD300) in combination with the respective group (ADHD, controls). Time point zero denotes the time point of STOP stimulus presentation. The scalp topographies for the ADHD and the control group are shown for the different condition (SCD0, SCD300). In the scalp topographies, blue colors show negativity, red colors denote positivity. The topographies are shown for the maximum amplitudes in the respective time windows for peak quantification as outlined in the methods section. The sLORETA plots show activation differences between the groups in the SCD300 condition in the inferior parietal cortex (corrected for multiple comparisons). The sLORETA color scale shows critical t-values.

Further post-hoc *t*-tests revealed that there was no difference between ADHD patients and controls in the SCD0 condition ($t(64) = 0.28$;

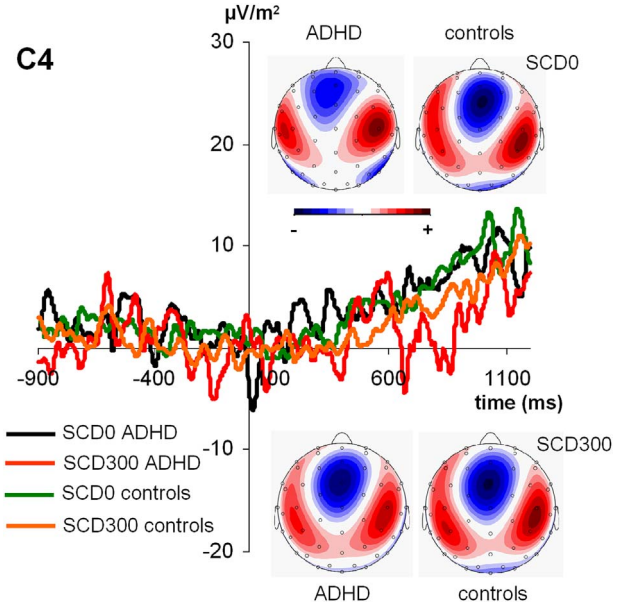

Fig. 5. RIDE R-cluster data at electrodes C4. The data are shown pooled across the uni-modal and the bi-modal condition, because there was no difference between these. The different line colors denote the different experimental conditions (SCD0, SCD300) in combination with the respective group (ADHD, controls). Time point zero denotes the time point of STOP stimulus presentation. The scalp topographies for the ADHD and the control group are shown for the different condition (SCD0, SCD300). In the scalp topographies, blue colors show negativity, red colors denote positivity. The topographies are shown for the maximum amplitudes in the respective time windows for peak quantification as outlined in the methods section.

$p > 0.8$), but that this was the case in the SCD300 condition ($t(64) = 5.35$; $p < 0.001$), where the C-cluster was larger in controls (35.39 $\mu V/m^2 \pm 2.1$) than in ADHD patients (19.79 $\mu V/m^2 \pm 2.1$). The source localization analysis using sLORETA revealed that this was due to activation differences in the left inferior parietal cortex including the temporo-parietal junction (TPJ) (BA40) (contrast: controls > ADHD patients). Concerning the R-cluster, shown in Fig. 5, no main or interaction effects were significant (all $F < 0.26$; $p > 0.6$).

As already done for the behavioral data, we used the medication status (i.e. the compound used) a covariate, to control for the effects of medication. These analyses show that the addition of this covariate did not alter the main or interaction effects found in above analyses and there was also no effect of the covariate itself (all $F < 0.49$; $p > 0.7$). It is also shown that the ADHD patients taking medication did not differ from the patients taking no medication, when the ADHD patient group was split (all $F < 0.65$; $p > 0.7$).

4. Discussion

In the current study we examined multi-component behavior in early adolescent patients with ADHD and healthy controls. The behavioral data show that early adolescent ADHD patients performed worse than controls when stimuli signalling the different required actions (i.e. stopping and changing) were temporally separated; early adolescent ADHD patients committed more response errors and showed longer RTs. In contrast to the initial hypothesis, however, this deficit was not further modulated by the complexity of sensory information to be used for multi-component behavior. This was supported by the Bayesian analysis. The reason for this lack of effects of the sensory modality may be that (i) the bi-modal condition led to a general floor effect in both groups or that (ii) multisensory integration deficits in early adolescent patients with ADHD represent a comorbidity rather than an inherent symptom of the disorder (Dionne-Dostie et al., 2015). In future studies it could be useful to screen for multisensory integration problems and to only include participants in whom such problems have been reported. Behavioral performance deficits seen in multi-component behavior in ADHD are therefore independent of the complexity of sensory information (i.e. uni-modal vs. bi-modal information) but are modulated by temporal factors.

As expected, the neurophysiological processes reflecting the behavioral effects could not be detected using standard ERP analyses because no interactions in line with the behavioral effects were observed. However, only after conducting residue iteration decomposition (RIDE) to account for intra-individual variability in neurophysiological data, we could show modulation of neurophysiological data in line with the behavioral data. Only the C-cluster, but not the S-cluster and R-cluster data reflect modulations in line with the behavioral data. The lack of differential group modulations in the S-cluster and R-cluster data was reflected in the Bayesian analysis. This dissociation suggests that deficits in multi-component behavior in early adolescent ADHD are not due to stimulus (attentional) processes, or processes related to motor response execution as reflected by the S and R-cluster (Ouyang et al., 2011). The important clinical implication is that the attentional dimension in ADHD is less important than the cognitive control/executive functions dimension for multi-component behavior and hence situations of high relevance for daily life competencies. This is of direct relevance for standard, clinical neuropsychological diagnostic procedures in which the attentional domain is still mainly focused. Actually, previous results suggest that the C-cluster reflects response selection processes which are usually indicated by the P3 ERP-component (Ouyang et al., 2017; Wolff et al., 2017). Importantly, response selection processes reflected by the C-cluster are subject to strong intra-individual modulations in ADHD (Bluschke et al., 2017). The P3 ERP-component has repeatedly been shown to reflect response selection mechanisms that bind stimulus encoding and responding (Mückschel et al., 2014; Petruo et al., 2016; Twomey et al., 2015; Verleger et al., 2005). These processes critically underlie performance in multi-component behavior (Beste et al., 2014; Mückschel et al., 2014). The finding that modulations were not observed for the P3 ERP-component, but for the C-cluster clearly shows that intra-individual variability in the neurophysiological data hampered the detection of neurophysiological mechanisms underlying multi-component behavior in early adolescent ADHD. The lower C-cluster amplitudes in early adolescent ADHD in the SCD300 condition suggest that ADHD patients have difficulties in performing stimulus-response bindings during multi-component behavior. The fact that this was only the case in the SCD300 condition, but not in the SCD0 condition, suggests that the temporal spacing of information detailing stimulus-response mappings determines the efficiency of stimulus-response bindings during multi-component behavior in early adolescent ADHD (Marusich and Gilden, 2014). It has been shown that adolescents have smaller time windows for efficient stimulus-response binding processes during multi-component behavior (Gohil et al., 2017b). However, in healthy participants such temporal windows for information integration have been suggested to be important for multi-sensory stimuli (Conrey and Pisoni, 2006; van Wassenhove et al., 2007), but irrelevant during uni-modal stimulus processing (Gori et al., 2008; Hahn et al., 2014; Hillock-Dunn et al., 2016). The current results suggest that there is a critical temporal integration window during multi-component behavior in early adolescent ADHD, which is (i) smaller than in healthy controls (Marusich and Gilden, 2014) and is (ii) independent of the nature and complexity of sensory input to be used during response selection. This has important clinical implication, because these results suggest that deficits in ADHD to cope with multiple demands are not determined by the sensory complexity. Rather, the time window seems to be critically changed in ADHD. It is possible that a 'critical temporal information integration' window may be useful to assess the severity of ADHD symptoms and may also provide a measure to evaluate effects of interventional trials. The finding that these aspects relate to functions of the TPJ (BA40) seems reasonable, because the TPJ has previously been found to be associated with modulations in the C-cluster (Wolff et al., 2017).

Moreover, the TPJ is involved in multi-component behavior (Duncan, 2010; Mückschel et al., 2014; Wu et al., 2017) and has also been shown to play in role in the chaining of actions during response selection (Chersi et al., 2011), as it sustains executive control (Collette et al., 2005). In the same line, the TPJ has been suggested to be involved in updating processes task representations (Geng and Vossel, 2013), which is important for the activation of different action goals during multi-component behavior. Since the TPJ shows structural abnormalities in ADHD (Brieber et al., 2007) it may be speculated that the deficits observed may reflect a consequence of structural neuroanatomical changes in ADHD. This nexus shall be investigated in more detail.

This study may be limited by the fact that the medication status within the ADHD group was heterogeneous. Moreover, since all testings were performed in the afternoon (~4 pm) and the used drugs have a relatively short half-life, medication should only have a minimal effect in the ADHD group. Importantly, the analyses including medication status as a factor, or when the ADHD group was split clearly showed that this aspect does not seem to affect the pattern of obtained results. The heterogeneous medication profile does therefore not impose strong limitations on the study. However, different ADHD subtypes were not compared and it is unclear in how far multisensory integration performance may be affected outside the applied paradigm. This limiting factor may be investigated in the future. However, the results obtained show strong effect sizes and the specificity of effects was confirmed using a Bayesian analysis of the data.

In summary, the study shows that multi-component behavior, an important faculty allowing the performance of everyday activities that require the hierarchical organization and processing of several individual actions, is not per se dysfunctional in early adolescent ADHD. The results suggest that there is critical temporal integration window during multi-component behavior in early adolescent ADHD, which is (i) smaller than in healthy controls but is (ii) independent of the complexity of sensory input to be used during response selection. These aspects specifically affect stimulus-response binding/selection processes associated with the inferior parietal cortex (BA40) and do not seem to affect perceptual/attentional gating and motor response processes.

Supplementary data to this article can be found online at https://doi.org/10.1016/j.nicl.2018.02.024.

Acknowledgements

This work was supported by a Grant from the Deutsche Forschungsgemeinschaft (DFG) BE4045/10-2.

References

Bekker, E.M., Overtoom, C.C., Kenemans, J.L., Kooij, J.J., De Noord, I., Buitelaar, J.K., Verbaten, M.N., 2005. Stopping and changing in adults with ADHD. Psychol. Med. 35, 807–816.

Beste, C., Saft, C., 2015. Action selection in a possible model of striatal medium spiny neuron dysfunction: behavioral and EEG data in a patient with benign hereditary chorea. Brain Struct. Funct. 220, 221–228. http://dx.doi.org/10.1007/s00429-013-0649-9.

Beste, C., Stock, A.-K., Epplen, J.T., Arning, L., 2014. On the relevance of the NPY2-receptor variation for modes of action cascading processes. NeuroImage 102 (Pt 2), 558–564. http://dx.doi.org/10.1016/j.neuroimage.2014.08.026.

Bluschke, A., Roessner, V., Beste, C., 2016. Specific cognitive-neurophysiological processes predict impulsivity in the childhood attention-deficit/hyperactivity disorder combined subtype. Psychol. Med. 46, 1277–1287. http://dx.doi.org/10.1017/S0033291715002822.

Bluschke, A., Chmielewski, W.X., Mückschel, M., Roessner, V., Beste, C., 2017. Neuronal intra-individual variability masks response selection differences between ADHD subtypes—a need to change perspectives. Front. Hum. Neurosci. 11. http://dx.doi.org/10.3389/fnhum.2017.00329.

Bodmer, B., Mückschel, M., Roessner, V., Beste, C., 2017. Neurophysiological variability masks differences in functional neuroanatomical networks and their effectiveness to modulate response inhibition between children and adults. Brain Struct. Funct. http://dx.doi.org/10.1007/s00429-017-1589-6.

Bos, D.J., Oranje, B., Achterberg, M., Vlaskamp, C., Ambrosino, S., de Reus, M.A., van den Heuvel, M.P., Rombouts, S.A.R.B., Durston, S., 2017. Structural and functional connectivity in children and adolescents with and without attention deficit/hyperactivity disorder. J. Child Psychol. Psychiatry 58, 810–818. http://dx.doi.org/10.1111/jcpp.12712.

Brieber, S., Neufang, S., Bruning, N., Kamp-Becker, I., Remschmidt, H., Herpertz-Dahlmann, B., Fink, G.R., Konrad, K., 2007. Structural brain abnormalities in adolescents with autism spectrum disorder and patients with attention deficit/hyperactivity disorder. J. Child Psychol. Psychiatry 48, 1251–1258. http://dx.doi.org/10.1111/j.1469-7610.2007.01799.x.

Chersi, F., Ferrari, P.F., Fogassi, L., 2011. Neuronal chains for actions in the parietal lobe: a computational model. PLoS One 6, e27652. http://dx.doi.org/10.1371/journal.pone.0027652.

Collette, F., Olivier, L., Van der Linden, M., Laureys, S., Delfiore, G., Luxen, A., Salmon, E., 2005. Involvement of both prefrontal and inferior parietal cortex in dual-task performance. Brain Res. Cogn. Brain Res. 24, 237–251. http://dx.doi.org/10.1016/j.cogbrainres.2005.01.023.

Conrey, B., Pisoni, D.B., 2006. Auditory-visual speech perception and synchrony detection for speech and nonspeech signals. J. Acoust. Soc. Am. 119, 4065–4073.

Diederich, A., Colonius, H., 2009. Crossmodal interaction in speeded responses: time window of integration model. Prog. Brain Res. 174, 119–135. http://dx.doi.org/10.1016/S0079-6123(09)01311-9.

Dionne-Dostie, E., Paquette, N., Lassonde, M., Gallagher, A., 2015. Multisensory integration and child neurodevelopment. Brain Sci. 5, 32–57. http://dx.doi.org/10.3390/brainsci5010032.

Dippel, G., Beste, C., 2015. A causal role of the right inferior frontal cortex in implementing strategies for multi-component behaviour. Nat. Commun. 6 (6587). http://dx.doi.org/10.1038/ncomms7587.

Doehnert, M., Brandeis, D., Schneider, G., Drechsler, R., Steinhausen, H.-C., 2013. A neurophysiological marker of impaired preparation in an 11-year follow-up study of attention-deficit/hyperactivity disorder (ADHD). J. Child Psychol. Psychiatry 54, 260–270. http://dx.doi.org/10.1111/j.1469-7610.2012.02572.x.

Döpfner, M., Görtz-Dorten, A., Lehmkuhl, G., 2008. Diagnostik-System für Psychische Störungen im Kindes- und Jugendalter nach ICD-10 und DSM-IV, DISYPS-II. Huber, Bern.

Downes, M., Bathelt, J., De Haan, M., 2017. Event-related potential measures of executive functioning from preschool to adolescence. Dev. Med. Child Neurol. 59, 581–590. http://dx.doi.org/10.1111/dmcn.13395.

Duncan, J., 2010. The multiple-demand (MD) system of the primate brain: mental programs for intelligent behaviour. Trends Cogn. Sci. http://dx.doi.org/10.1016/j.tics.2010.01.004.

Fuchs, M., Kastner, J., Wagner, M., Hawes, S., Ebersole, J.S., 2002. A standardized boundary element method volume conductor model. Clin. Neurophysiol. 113, 702–712.

Geng, J.J., Vossel, S., 2013. Re-evaluating the role of TPJ in attentional control: contextual updating? Neurosci. Biobehav. Rev. 37, 2608–2620. http://dx.doi.org/10.1016/j.neubiorev.2013.08.010.

Gohil, K., Stock, A.-K., Beste, C., 2015. The importance of sensory integration processes for action cascading. Sci. Rep. 5 (9485). http://dx.doi.org/10.1038/srep09485.

Gohil, K., Bluschke, A., Roessner, V., Stock, A.-K., Beste, C., 2017a. ADHD patients fail to maintain task goals in face of subliminally and consciously induced cognitive conflicts. Psychol. Med. 1–13. http://dx.doi.org/10.1017/S0033291717000216.

Gohil, K., Bluschke, A., Roessner, V., Stock, A.-K., Beste, C., 2017b. Sensory processes modulate differences in multi-component behavior and cognitive control between childhood and adulthood. Hum. Brain Mapp. 38, 4933–4945. http://dx.doi.org/10.1002/hbm.23705.

Gori, M., Del Viva, M., Sandini, G., Burr, D.C., 2008. Young children do not integrate visual and haptic form information. Curr. Biol. 18, 694–698. http://dx.doi.org/10.1016/j.cub.2008.04.036.

Hahn, N., Foxe, J.J., Molholm, S., 2014. Impairments of multisensory integration and cross-sensory learning as pathways to dyslexia. Neurosci. Biobehav. Rev. 47, 384–392. http://dx.doi.org/10.1016/j.neubiorev.2014.09.007.

Heinrich, H., Grunitz, J., Stonawski, V., Frey, S., Wahl, S., Albrecht, B., Goecke, T.W., Beckmann, M.W., Kornhuber, J., Fasching, P.A., Moll, G.H., Eichler, A., 2017. Attention, cognitive control and motivation in ADHD: linking event-related brain potentials and DNA methylation patterns in boys at early school age. Sci. Rep. 7 (3823). http://dx.doi.org/10.1038/s41598-017-03326-3.

Henríquez-Henríquez, M.P., Billeke, P., Henríquez, H., Zamorano, F.J., Rothhammer, F., Aboitiz, F., 2014. Intra-individual response variability assessed by ex-Gaussian analysis may be a new endophenotype for attention-deficit/hyperactivity disorder. Front. Psych. 5, 197. http://dx.doi.org/10.3389/fpsyt.2014.00197.

Hillock-Dunn, A., Grantham, D.W., Wallace, M.T., 2016. The temporal binding window for audiovisual speech: children are like little adults. Neuropsychologia 88, 74–82. http://dx.doi.org/10.1016/j.neuropsychologia.2016.02.017.

Hoogman, M., Bralten, J., Hibar, D.P., Mennes, M., Zwiers, M.P., Schweren, L.S.J., van Hulzen, K.J.E., Medland, S.E., Shumskaya, E., Jahanshad, N., de Zeeuw, P., Szekely, E., Sudre, G., Wolfers, T., Onnink, A.M.H., Dammers, J.T., Mostert, J.C., Vives-Gilabert, Y., Kohls, G., Oberwelland, E., Seitz, J., Schulte-R?ther, M., Ambrosino, S., Doyle, A.E., H?vik, M.F., Dramsdahl, M., Tamm, L., van Erp, T.G.M., Dale, A., Schork, A., Conzelmann, A., Zierhut, K., Baur, R., McCarthy, H., Yoncheva, Y.N., Cubillo, A., Chantiluke, K., Mehta, M.A., Paloyelis, Y., Hohmann, S., Baumeister, S., Bramati, I., Mattos, P., Tovar-Moll, F., Douglas, P., Banaschewski, T., Brandeis, D., Kuntsi, J., Asherson, P., Rubia, K., Kelly, C., Martino, A.D., Milham, M.P., Castellanos, F.X., Frodl, T., Zentis, M., Lesch, K.-P., Reif, A., Pauli, P., Jernigan, T.L., Haavik, J., Plessen, K.J., Lundervold, A.J., Hugdahl, K., Seidman, L.J., Biederman, J., Rommelse, N., Heslenfeld, D.J., Hartman, C.A., Hoekstra, P.J., Oosterlaan, J., von Polier, G., Konrad, K., Vilarroya, O., Ramos-Quiroga, J.A., Soliva, J.C., Durston, S., Buitelaar, J.K., Faraone, S.V., Shaw, P., Thompson, P.M., Franke, B., 2017. Subcortical brain

volume differences in participants with attention deficit hyperactivity disorder in children and adults: a cross-sectional mega-analysis. Lancet Psych. 4, 310–319. http://dx.doi.org/10.1016/S2215-0366(17)30049-4.
Kenemans, J.L., Bekker, E.M., Lijffijt, M., Overtoom, C.C.E., Jonkman, L.M., Verbaten, M.N., 2005. Attention deficit and impulsivity: selecting, shifting, and stopping. Int. J. Psychophysiol. 58, 59–70. http://dx.doi.org/10.1016/j.ijpsycho.2005.03.009.
Letzner, S., Güntürkün, O., Beste, C., 2017. How birds outperform humans in multi-component behavior. Curr. Biol. CB 27, R996–R998. http://dx.doi.org/10.1016/j.cub.2017.07.056.
Lin, H.-Y., Hwang-Gu, S.-L., Gau, S.S.-F., 2015. Intra-individual reaction time variability based on ex-Gaussian distribution as a potential endophenotype for attention-deficit/hyperactivity disorder. Acta Psychiatr. Scand. 132, 39–50. http://dx.doi.org/10.1111/acps.12393.
Mackie, M.-A., Van Dam, N.T., Fan, J., 2013. Cognitive control and attentional functions. Brain Cogn. 82, 301–312. http://dx.doi.org/10.1016/j.bandc.2013.05.004.
Marco-Pallarés, J., Grau, C., Ruffini, G., 2005. Combined ICA-LORETA analysis of mismatch negativity. NeuroImage 25, 471–477. http://dx.doi.org/10.1016/j.neuroimage.2004.11.028.
Marusich, L.R., Gilden, D.L., 2014. Assessing temporal integration spans in ADHD through apparent motion. Neuropsychology 28, 585–593. http://dx.doi.org/10.1037/neu0000080.
Masson, M.E.J., 2011. A tutorial on a practical Bayesian alternative to null-hypothesis significance testing. Behav. Res. Methods 43, 679–690. http://dx.doi.org/10.3758/s13428-010-0049-5.
Meredith, M.A., 2002. On the neuronal basis for multisensory convergence: a brief overview. Brain Res. Cogn. Brain Res. 14, 31–40.
Mückschel, M., Stock, A.-K., Beste, C., 2014. Psychophysiological mechanisms of inter-individual differences in goal activation modes during action cascading. Cereb. Cortex 24, 2120–2129. http://dx.doi.org/10.1093/cercor/bht066.
Mückschel, M., Stock, A.-K., Beste, C., 2015. Different strategies, but indifferent strategy adaptation during action cascading. Sci. Rep. 5. http://dx.doi.org/10.1038/srep09992.
Nejati, V., Salehinejad, M.A., Nitsche, M.A., Najian, A., Javadi, A.-H., 2017. Transcranial direct current stimulation improves executive dysfunctions in ADHD: implications for inhibitory control, interference control, working memory, and cognitive flexibility. J. Atten. Disord. http://dx.doi.org/10.1177/1087054717730611.
Ness, V., Beste, C., 2013. The role of the striatum in goal activation of cascaded actions. Neuropsychologia 51, 2562–2571. http://dx.doi.org/10.1016/j.neuropsychologia.2013.09.032.
Nunez, P.L., Pilgreen, K.L., 1991. The spline-Laplacian in clinical neurophysiology: a method to improve EEG spatial resolution. J. Clin. Neurophysiol. 8, 397–413.
Ouyang, G., Herzmann, G., Zhou, C., Sommer, W., 2011. Residue iteration decomposition (RIDE): a new method to separate ERP components on the basis of latency variability in single trials. Psychophysiology 48, 1631–1647. http://dx.doi.org/10.1111/j.1469-8986.2011.01269.x.
Ouyang, G., Sommer, W., Zhou, C., 2015a. Updating and validating a new framework for restoring and analyzing latency-variable ERP components from single trials with residue iteration decomposition (RIDE). Psychophysiology 52, 839–856. http://dx.doi.org/10.1111/psyp.12411.
Ouyang, G., Sommer, W., Zhou, C., 2015b. A toolbox for residue iteration decomposition (RIDE)—a method for the decomposition, reconstruction, and single trial analysis of event related potentials. J. Neurosci. Methods 250, 7–21. http://dx.doi.org/10.1016/j.jneumeth.2014.10.009.
Ouyang, G., Hildebrandt, A., Sommer, W., Zhou, C., 2017. Exploiting the intra-subject latency variability from single-trial event-related potentials in the P3 time range: a review and comparative evaluation of methods. Neurosci. Biobehav. Rev. 75, 1–21. http://dx.doi.org/10.1016/j.neubiorev.2017.01.023.
Pascual-Marqui, R.D., 2002. Standardized low-resolution brain electromagnetic tomography (sLORETA): technical details. Methods Find. Exp. Clin. Pharmacol. 24 (Suppl D), 5–12.
Petruo, V.A., Stock, A.-K., Münchau, A., Beste, C., 2016. A systems neurophysiology approach to voluntary event coding. NeuroImage 135, 324–332. http://dx.doi.org/10.1016/j.neuroimage.2016.05.007.
Raftery, A.E., 1995. Bayesian model selection in social research. Sociol. Methodol. 25, 111. http://dx.doi.org/10.2307/271063.
Rommel, A.-S., James, S.-N., McLoughlin, G., Brandeis, D., Banaschewski, T., Asherson, P., Kuntsi, J., 2017. Association of preterm birth with attention-deficit/hyperactivity disorder-like and wider-ranging neurophysiological impairments of attention and inhibition. J. Am. Acad. Child Adolesc. Psychiatry 56, 40–50. http://dx.doi.org/10.1016/j.jaac.2016.10.006.
Saville, C.W.N., Feige, B., Kluckert, C., Bender, S., Biscaldi, M., Berger, A., Fleischhaker, C., Henighausen, K., Klein, C., 2015. Increased reaction time variability in attention-deficit hyperactivity disorder as a response-related phenomenon: evidence from single-trial event-related potentials. J. Child Psychol. Psychiatry 56, 801–813. http://dx.doi.org/10.1111/jcpp.12348.
Sebastian, A., Jung, P., Krause-Utz, A., Lieb, K., Schmahl, C., Tüscher, O., 2014. Frontal dysfunctions of impulse control - a systematic review in borderline personality disorder and attention-deficit/hyperactivity disorder. Front. Hum. Neurosci. 8 (698). http://dx.doi.org/10.3389/fnhum.2014.00698.
Sekihara, K., Sahani, M., Nagarajan, S.S., 2005. Localization bias and spatial resolution of adaptive and non-adaptive spatial filters for MEG source reconstruction. NeuroImage 25, 1056–1067. http://dx.doi.org/10.1016/j.neuroimage.2004.11.051.
Sonuga-Barke, E.J.S., Cortese, S., Fairchild, G., Stringaris, A., 2016. Annual research review: transdiagnostic neuroscience of child and adolescent mental disorders—differentiating decision making in attention-deficit/hyperactivity disorder, conduct disorder, depression, and anxiety. J. Child Psychol. Psychiatry 57, 321–349. http://dx.doi.org/10.1111/jcpp.12496.
Stock, A.-K., Arning, L., Epplen, J.T., Beste, C., 2014. DRD1 and DRD2 genotypes modulate processing modes of goal activation processes during action cascading. J. Neurosci. 34, 5335–5341. http://dx.doi.org/10.1523/JNEUROSCI.5140-13.2014.
Tao, J., Jiang, X., Wang, X., Liu, H., Qian, A., Yang, C., Chen, H., Li, J., Ye, Q., Wang, J., Wang, M., 2017. Disrupted control-related functional brain networks in drug-naive children with attention-deficit/hyperactivity disorder. Front. Psych. 8 (246). http://dx.doi.org/10.3389/fpsyt.2017.00246.
Thomas, R., Sanders, S., Doust, J., Beller, E., Glasziou, P., 2015. Prevalence of attention-deficit/hyperactivity disorder: a systematic review and meta-analysis. Pediatrics 135, e994–1001. http://dx.doi.org/10.1542/peds.2014-3482.
Twomey, D.M., Murphy, P.R., Kelly, S.P., O'Connell, R.G., 2015. The classic P300 encodes a build-to-threshold decision variable. Eur. J. Neurosci. 42, 1636–1643. http://dx.doi.org/10.1111/ejn.12936.
Tye, C., Asherson, P., Ashwood, K.L., Azadi, B., Bolton, P., McLoughlin, G., 2014. Attention and inhibition in children with ASD, ADHD and co-morbid ASD + ADHD: an event-related potential study. Psychol. Med. 44, 1101–1116. http://dx.doi.org/10.1017/S0033291713001049.
Verbruggen, F., Schneider, D.W., Logan, G.D., 2008. How to stop and change a response: the role of goal activation in multitasking. J. Exp. Psychol. Hum. Percept. Perform. 34, 1212–1228. http://dx.doi.org/10.1037/0096-1523.34.5.1212.
Verleger, R., Jaśkowski, P., Wascher, E., 2005. Evidence for an integrative role of P3b in linking reaction to perception. J. Psychophysiol. 19, 165–181. http://dx.doi.org/10.1027/0269-8803.19.3.165.
Verleger, R., Metzner, M.F., Ouyang, G., Śmigasiewicz, K., Zhou, C., 2014. Testing the stimulus-to-response bridging function of the oddball-P3 by delayed response signals and residue iteration decomposition (RIDE). NeuroImage 100, 271–280. http://dx.doi.org/10.1016/j.neuroimage.2014.06.036.
Wagenmakers, E.-J., 2007. A practical solution to the pervasive problems of p values. Psychon. Bull. Rev. 14, 779–804.
van Wassenhove, V., Grant, K.W., Poeppel, D., 2007. Temporal window of integration in auditory-visual speech perception. Neuropsychologia 45, 598–607. http://dx.doi.org/10.1016/j.neuropsychologia.2006.01.001.
Wolff, N., Mückschel, M., Beste, C., 2017. Neural mechanisms and functional neuroanatomical networks during memory and cue-based task switching as revealed by residue iteration decomposition (RIDE) based source localization. Brain Struct. Funct. 222, 3819–3831. http://dx.doi.org/10.1007/s00429-017-1437-8.
Wu, T., Dufford, A.J., Egan, L.J., Mackie, M.-A., Chen, C., Yuan, C., Chen, C., Li, X., Liu, X., Hof, P.R., Fan, J., 2017. Hick-Hyman Law is mediated by the cognitive control network in the brain. Cereb. Cortex 1991 1–16. http://dx.doi.org/10.1093/cercor/bhx127.